

Lattice calculations of D_s to η and η' decay form factors

Issaku Kanamori*

Institut für Theoretische Physik, University of Regensburg, D-93040 Regensburg, Germany

E-mail: issaku.kanamori@physik.uni-regensburg.de

We report on lattice results of the form factors for semi-leptonic decays of the D_s meson to η and η' , with $n_f = 2 + 1$ configurations. The calculation contains disconnected fermion loop diagrams, which are challenging to calculate on the lattice. Our result shows that the disconnected diagrams give significant contributions to the form factors.

Xth Quark Confinement and the Hadron Spectrum

8-12 October 2012

TUM Campus Garching, Munich, Germany

*Speaker.

1. Introduction

About 15% of the decays of the D_s meson are semi-leptonic. There are by far dominated by decays with η , η' and ϕ mesons in the final state. The decays into η and η' contain interesting flavor physics, in particular, the mixing of η and η' . Investigating the corresponding form factors helps to understand the magnitude of the gluonic contribution to η' (see [1], for example). The mixing can be studied through both D and D_s semi-leptonic decays. However, the latter is easier to access in experiment, since it is a Cabibbo allowed process.

The $D_s \rightarrow \eta^{(\prime)}$ semi-leptonic decays are characterized by the following two form factors, $f_0(q^2)$ and $f_+(q^2)$:

$$\langle \eta^{(\prime)}(k) | V^\mu(q^2) | D_s(p) \rangle = f_+(q^2) \left[(p+k)^\mu - \frac{M_{D_s}^2 - M_{\eta^{(\prime)}}^2}{q^2} q^\mu \right] + f_0(q^2) \frac{M_{D_s}^2 - M_{\eta^{(\prime)}}^2}{q^2} q^\mu, \quad (1.1)$$

where V^μ is a vector current and M_{D_s} and $M_{\eta^{(\prime)}}$ are the masses of D_s and $\eta^{(\prime)}$, respectively. Together with the CKM matrix, one can relate the form factors to the decay width and thus the branching ratio. Experimental results for these decay modes are starting to appear, see [2, 3]. The matrix element (l.h.s) is what we can obtain from the lattice. We will focus only on the scalar form factor $f_0(q^2)$, which can be related to the scalar matrix element [4]

$$f_0(q^2) = \frac{m_c - m_s}{M_{D_s}^2 - M_{\eta^{(\prime)}}^2} \langle \eta^{(\prime)} | S | D_s \rangle, \quad (1.2)$$

where $S = \bar{s}c$, and m_s and m_c are the s - and c -quark masses, respectively. This relation has an advantage over eq. (1.1), in the sense that it does not require the current renormalization.

Currently, only a prediction of the form factors from the light cone sum rules is available [5]. A first principles calculation on the lattice is desirable. It also provides an interesting playground for quantum field theory, since physics relevant to η' should contain non-trivial effects from the chiral anomaly as characterized by the Veneziano-Witten formula [6, 7].

However, a lattice calculation of the decay form factor is technically challenging, as it requires the evaluation of disconnected fermion loop diagrams. In order to obtain the relevant matrix elements, we need to compute the following three point functions shown pictorially:

$$\langle \eta^{(\prime)}(\vec{k}) | S(\vec{q}) | D_s(\vec{p}) \rangle = \text{Diagram 1} - \sum_{l=u,d,s} \left(\text{Diagram 2} + \text{Diagram 3} \right), \quad (1.3)$$

where the solid lines represent fermion propagators. The first and the second terms are the connected and disconnected fermion loop diagrams, respectively. Note that the disconnected one is in fact connected by gluons. We expect to see the effect of the anomaly in the pseudoscalar flavor singlet sector and this is only possible with the disconnected terms.

To obtain a fermion propagator, we need to invert the Dirac operator, a matrix of typically $O(10^7) \times O(10^7)$. Many of the quark propagators in the three point function appearing in eq. (1.3) only require a few columns of the inverted matrices. However, the disconnected diagram requires the whole inverted matrix (i.e. an all-to-all propagator) for the light quarks (l) and thus is computationally much more expensive to calculate. Note that the disconnected contributions are summed

over the three light flavors, which enhances the contributions by roughly a factor of three. This is another reason to expect that they may be large.

Although the calculation is challenging, it is still feasible [8]. We use stochastic estimations of all-to-all propagators in the disconnected fermion diagrams. In addition, we also use the stochastic method for the charm quark propagator in the connected diagram (denoted by a blue line in eq. (1.3)) [9]. This allows us to access many different momentum combinations, which helps to improve the signal by averaging over rotationally equivalent momenta. The stochastic estimations introduce stochastic noise in addition to gauge noise, and we combine several noise reduction techniques, such as the standard low mode averaging and the truncated solver method (TSM) [10].

To carry out the lattice calculation, we use QCDSF $n_f = 2 + 1$ configurations [11, 12]. The strategy of these sets of configurations is to keep the flavor singlet mass average of the three quarks, $\frac{1}{3}(m_u + m_d + m_s)$, constant. Starting from the flavor SU(3) symmetric point, $m_{u,d} = m_s$, $m_{u,d}$ is reduced and m_s is increased. This setup is ideal to study flavor physics in the SU(3) flavor basis. So far, we have analyzed 939 configurations at the flavor symmetric point, corresponding to pion and Kaon masses $M_\pi = M_K = 450\text{MeV}$, and 239 configurations with $M_\pi = 348\text{MeV}$ and $M_K = 483\text{MeV}$. The physical spacial extent of the lattice is roughly 1.9fm , and the lattice spacing is $a \sim 0.08\text{fm}$ for both sets of configurations. The stout link non-perturbatively improved clover action (SLiNC) [13], for which the discretization effects are removed to $O(a)$, is used for both the dynamical u , d and s -quarks and the partially quenched c -quark,

In the next section, we extract the masses of η and η' , and a mixing angle between the SU(3) flavor singlet-octet basis and the physical states. We then present our result for the scalar form factor f_0 in section 3.

2. Extracting η and η'

Since the configurations are well suited to study the effects of flavor symmetry breaking, we start with the following SU(3) basis to describe η and η' :

$$\eta_8 = \frac{1}{\sqrt{6}}(u\bar{u} + d\bar{d} - 2s\bar{s}), \quad \eta_1 = \frac{1}{\sqrt{3}}(u\bar{u} + d\bar{d} + s\bar{s}). \quad (2.1)$$

The physical η and η' should be a mixing of the above octet state (η_8) and the singlet state (η_1):

$$\eta = \cos \theta \eta_8 - \sin \theta \eta_1, \quad \eta' = \sin \theta \eta_8 + \cos \theta \eta_1. \quad (2.2)$$

We use a single angle parameterization and do not include a gluonic state in eq. (2.2), since we expect the gluonic contributions to be small. In principle we can resolve the contribution but is beyond the current analysis. The interpolating operator $\mathcal{O}_{\eta^{(\prime)}}^\dagger$ that will be used creates an overlap with the $\eta^{(\prime)}$ state sufficient to obtain the target matrix elements.

To extract the η and η' states from the lattice data, we need to diagonalize the following 2×2 two point correlation matrix:

$$C_2(t; \vec{k}) = \begin{pmatrix} \langle \mathcal{O}_8(t; \vec{k}) \mathcal{O}_8^\dagger(0) \rangle & \langle \mathcal{O}_8(t; \vec{k}) \mathcal{O}_1^\dagger(0) \rangle \\ \langle \mathcal{O}_1(t; \vec{k}) \mathcal{O}_8^\dagger(0) \rangle & \langle \mathcal{O}_1(t; \vec{k}) \mathcal{O}_1^\dagger(0) \rangle \end{pmatrix}, \quad (2.3)$$

where \mathcal{O}_8 and \mathcal{O}_1 are interpolating operators for η_8 and η_1 , respectively, and t is the time separation between source and sink. The operators at the sink are projected to momentum \vec{k} . Here we use smeared interpolating operators (Wuppertal smearing [14]) to reduce the effects from the excited states. The diagonalized basis gives the operator $\mathcal{O}_{\eta^{(\prime)}}$ for physical $\eta^{(\prime)}$, and the diagonalized two point functions give the spectra for $t/a \gg 1$:

$$C_2^{\text{diag}, \eta}(t, \vec{k}) = \frac{|Z_{\eta, \vec{k}}|^2}{2E_{\eta, \vec{k}}} \exp(-E_{\eta, \vec{k}} t), \quad C_2^{\text{diag}, \eta'}(t, \vec{k}) = \frac{|Z_{\eta', \vec{k}}|^2}{2E_{\eta', \vec{k}}} \exp(-E_{\eta', \vec{k}} t), \quad (2.4)$$

where $Z_{\eta^{(\prime)}, \vec{k}} = \langle \eta^{(\prime)}(\vec{k}) | \mathcal{O}_{\eta^{(\prime)}}^\dagger(\vec{k}) | 0 \rangle$ is an overlap factor between the $\eta^{(\prime)}$ state with momentum \vec{k} and a state created by the interpolating operator. $E_{\eta^{(\prime)}, \vec{k}}$ is the energy of the state. Setting $\vec{k} = \vec{0}$, we obtain the masses. Note that each element in eq. (2.3) contains both connected and disconnected fermion loops. For example, the $\eta_8 \rightarrow \eta_8$ two point function contains the following fermion diagrams:

$$\langle \mathcal{O}_8(t; \vec{k}) \mathcal{O}_8^\dagger(0) \rangle = \frac{1}{3} \left[\begin{array}{c} \text{Diagram 1: } \text{light quark loop} \\ \text{Diagram 2: } 2 \times \text{strange quark loop} \\ \text{Diagram 3: } -2 \times (\text{light quark loop} \times \text{light quark loop}) \\ \text{Diagram 4: } -2 \times (\text{strange quark loop} \times \text{strange quark loop}) \\ \text{Diagram 5: } +2 \times (\text{light quark loop} \times \text{strange quark loop}) \\ \text{Diagram 6: } +2 \times (\text{strange quark loop} \times \text{light quark loop}) \end{array} \right],$$

where l stands for light (i.e., u - and d -) quarks. In figure 1, we show the effective mass plot

$$aM_{\text{eff}} \left(t + \frac{a}{2} \right) = \log \frac{C_2^{\text{diag}}(t)}{C_2^{\text{diag}}(t+a)} \quad (2.5)$$

for η and η' together with that of π . The figure demonstrates our ability to separate the η and η' states.

The diagonalization presented so far gives a mixing of the interpolating operators \mathcal{O}_1 and \mathcal{O}_8 , which depends on the smearing of our choice. To obtain the *physical* mixing, we replace the smeared operators at t in eq. (2.3) by local operators. The smeared operators are still used at $t = 0$ so we need to use $Z_{\eta^{(\prime)}}$ from smeared(source)-smeared(sink) two point functions to normalize the matrix elements. Setting the momentum $\vec{k} = \vec{0}$, we can extract the following matrix elements:

$$a_\eta^8 = \langle 0 | \mathcal{O}_8^{\text{local}} | \eta \rangle, \quad a_{\eta'}^8 = \langle 0 | \mathcal{O}_8^{\text{local}} | \eta' \rangle, \quad a_\eta^1 = \langle 0 | \mathcal{O}_1^{\text{local}} | \eta \rangle, \quad a_{\eta'}^1 = \langle 0 | \mathcal{O}_1^{\text{local}} | \eta' \rangle. \quad (2.6)$$

Modulo renormalization factors, they are proportional to the decay constants in the SU(3) flavor basis: for example, $Z_8 a_\eta^8 = M_\eta f_\eta^8$, where Z_8 is the renormalization factor and f_η^8 is the decay constant of η through the octet. We use the following ratio to obtain the mixing angle θ ,

$$\tan^2 \theta = \frac{\langle 0 | \mathcal{O}_1^{\text{local}} | \eta \rangle \langle 0 | \mathcal{O}_8^{\text{local}} | \eta' \rangle}{\langle 0 | \mathcal{O}_8^{\text{local}} | \eta \rangle \langle 0 | \mathcal{O}_1^{\text{local}} | \eta' \rangle}, \quad (2.7)$$

for which the renormalization factors cancel.

Figure 2 shows our preliminary values for the mass (left panel) and mixing angle (right panel) together with the experimental values and other lattice results. We find $M_\eta = 513(11) \text{ MeV}$, $M_{\eta'} = 750(130) \text{ MeV}$, and $\theta = -8.3^\circ(2.8)$ at $M_\pi = 348 \text{ MeV}$. Note that our result has no mixing by definition at the SU(3) flavor symmetric point: $\eta \equiv \eta_8$ and $\eta' \equiv \eta_1$. Currently, we have not yet included disconnected two point functions for this ensemble, which means $M_\eta = M_{\eta'}$

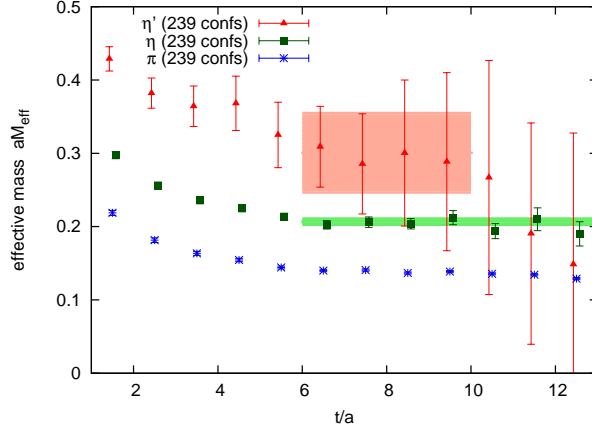


Figure 1: Effective mass plot for π , η , and η' for the $M_\pi = 348$ MeV ensemble.

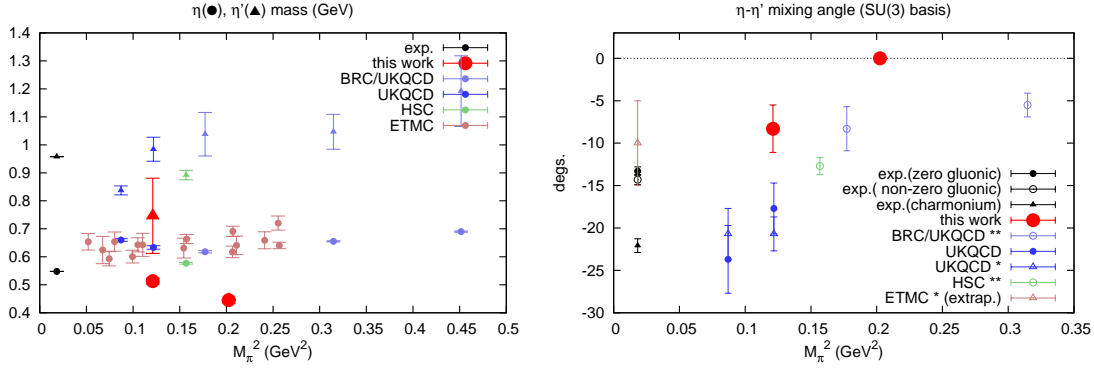


Figure 2: Summary of lattice results for the masses of η and η' (left panel) and the mixing angle (right panel). Included are result from the BRC/UKQCD [15], UKQCD [16], HSC [17], and ETMC [18] collaborations. For the mixing angle, two experimental values by KLOE [19] (\bullet , \circ) are from radiative decays ($\rho, \omega, \phi \rightarrow (\pi^0, \eta, \eta')\gamma$, $\eta' \rightarrow \rho\gamma$ and $(\pi^0, \eta') \rightarrow \gamma\gamma$); they assume zero (\bullet) and non-zero (\circ) gluonic contributions to η' state, respectively. The other experimental value (\blacktriangle) is from BES [20], which uses charmonium decays only. Data with * use both local and fuzzed (smeared) operators and ** fuzzed (smeared) operators only.

3. Decay Form Factors

Above we have constructed suitable interpolating operators for η and η' , so it is straightforward to obtain the matrix element we need from the following three point function:

$$C_3^{D_s \rightarrow \eta^{(\prime)}}(t) = \langle \mathcal{O}_{\eta^{(\prime)}}(t_f; \vec{k}) S(t; \vec{q}) \mathcal{O}_{D_s}^\dagger(t_i) \rangle$$

$$\xrightarrow{t_f \gg t \gg t_i} \frac{Z_{\eta^{(\prime)}, \vec{k}} Z_{D_s, \vec{p}}}{4E_{\eta^{(\prime)}, \vec{k}} E_{D_s, \vec{p}}} \exp \left[-E_{D_s, \vec{p}}(t - t_i) - E_{\eta^{(\prime)}, \vec{k}}(t_f - t) \right] \langle \eta^{(\prime)}(\vec{k}) | S(\vec{q}) | D_s(\vec{p}) \rangle. \quad (3.1)$$

Here, $\vec{p} = \vec{k} + \vec{q}$ and \mathcal{O}_{D_s} is an interpolating operator for D_s . We use a similar parameterization to eq. (2.4) for the two point function $\langle \mathcal{O}_{D_s}(t; \vec{p}) \mathcal{O}_{D_s}^\dagger(0) \rangle$. By combining eqs. (2.4), (3.1) and

$\langle \mathcal{O}_{D_s}(t; \vec{p}) \mathcal{O}_{D_s}^\dagger(0) \rangle$, we obtain the matrix element $\langle \eta^{(\prime)}(\vec{k}) | S(\vec{q}) | D_s(\vec{p}) \rangle$.

In figure 3, we plot our preliminary results for $f_0(q^2)$ for the SU(3) flavor symmetric case. A fit to the functional form $f_0(q^2) = \frac{f_0(0)}{1-bq^2}$ is also shown. We find $f_0(0) = 0.75(3)$ for $D_s \rightarrow \bar{l} \nu_l \eta$ and $f_0(0) = 0.52(5)$ for $D_s \rightarrow \bar{l} \nu_l \eta'$, at $M_\pi = 450$ MeV.

To calculate the three point functions, we included all disconnected fermion loops. As mentioned in the previous section, we have used the approximation $M_\eta = M_{\eta'}$ to compute the two point functions, which allows us to use different $t_{\text{sep}} = t_f - t_i$ in eq. (3.1) for the connected fermion loop contribution ($t_{\text{sep}} = 24a$) and the disconnected one ($t_{\text{sep}} = 8a$). A larger t_{sep} suppresses possible pollution from excited states, but leads to larger statistical errors, which is particularly problematic for the disconnected diagrams. Using different t_{sep} for the connected and disconnected three point functions circumvents these problems in this case. A full analysis with $M_\eta \neq M_{\eta'}$, which could affect the $D_s \rightarrow \bar{l} \nu_l \eta_1$ form factor, is currently under investigation. Due to flavor symmetry, the $D_s \rightarrow \bar{l} \nu_l \eta_8$ form factor is identical to $D \rightarrow \bar{l} \nu_l \pi$ and $D \rightarrow \bar{l} \nu_l K$ at the symmetric point ($M_\pi = 450$ MeV).

Interestingly, we find that the contributions from the disconnected fermion loops are significant, see figure 4 where both connected and disconnected contributions to $C_3^{D_s \rightarrow \eta'}(t)$ are plotted separately. The figure also indicates that the main source of the statistical error comes from the disconnected contribution.

The results presented here are still preliminary. In particular, the effects of excited states of the D_s and possibly η , η' are still under investigation. The effective mass plot (figure 1) suggests that the excited state may contribute up to $t/a \lesssim 5$. Since our fit region for the three point function is at most $1 \leq t/a \leq 7$ for the disconnected diagrams, there may be some pollution from excited states. Note that the effects of an excited state (e.g. η^*) to the two point functions is suppressed by a square of the overlapping factor. For example, including the leading order of the excited contributions eq. (2.4) becomes

$$C_2^{\text{diag}, \eta}(t, \vec{k}) = \frac{|Z_{\eta, \vec{k}}|^2}{2E_{\eta, \vec{k}}} \exp(-E_{\eta, \vec{k}} t) \left(1 + \frac{|Z_{\eta^*, \vec{k}}|^2}{|Z_{\eta, \vec{k}}|^2} \frac{E_{\eta, \vec{k}}}{E_{\eta^*, \vec{k}}} \exp[-(E_{\eta^*, \vec{k}} - E_{\eta, \vec{k}})t] + \dots \right). \quad (3.2)$$

The term $|Z_{\eta^*}/Z_\eta|^2$ appears as a correction. On the other hand, the pollution to the three point function is suppressed by only a linear factor:

$$\begin{aligned} C_3^{D_s \rightarrow \eta}(t) &= \frac{Z_{\eta, \vec{k}} Z_{D_s, \vec{p}}}{4E_{\eta, \vec{k}} E_{D_s, \vec{p}}} \exp[-E_{D_s, \vec{p}}(t - t_i) - E_{\eta^{(\prime)}, \vec{k}}(t_f - t)] \langle \eta(\vec{k}) | S(\vec{q}) | D_s(\vec{p}) \rangle \\ &\times \left[1 + \frac{Z_{\eta^*, \vec{k}}}{Z_{\eta, \vec{k}}} \frac{E_{\eta, \vec{k}}}{E_{\eta^*, \vec{k}}} \exp[-(E_{\eta^*, \vec{k}} - E_{\eta, \vec{k}})(t_f - t)] \frac{\langle \eta^*(\vec{k}) | S(\vec{q}) | D_s(\vec{p}) \rangle}{\langle \eta(\vec{k}) | S(\vec{q}) | D_s(\vec{p}) \rangle} \right. \\ &\quad \left. + \frac{Z_{D_s^*, \vec{p}}}{Z_{D_s, \vec{p}}} \frac{E_{D_s, \vec{p}}}{E_{D_s^*, \vec{p}}} \exp[-(E_{D_s^*, \vec{p}} - E_{D_s, \vec{p}})(t - t_i)] \frac{\langle \eta(\vec{k}) | S(\vec{q}) | D_s^*(\vec{p}) \rangle}{\langle \eta(\vec{k}) | S(\vec{q}) | D_s(\vec{p}) \rangle} + \dots \right], \quad (3.3) \end{aligned}$$

where the correction starts with the Z_{η^*}/Z_η term. It is important to remove these effects or to estimate their magnitude, which may be one of the main sources of the systematic error in our calculation.

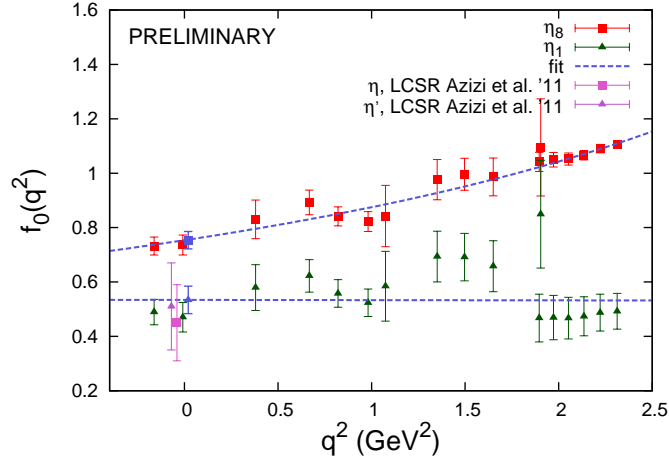


Figure 3: Preliminary results for the scalar form factor $f_0(q^2)$ for the SU(3) flavor symmetric ensemble ($M_\pi = 450\text{MeV}$). Also included are results from light cone QCD sum rules (LCSR) [5].

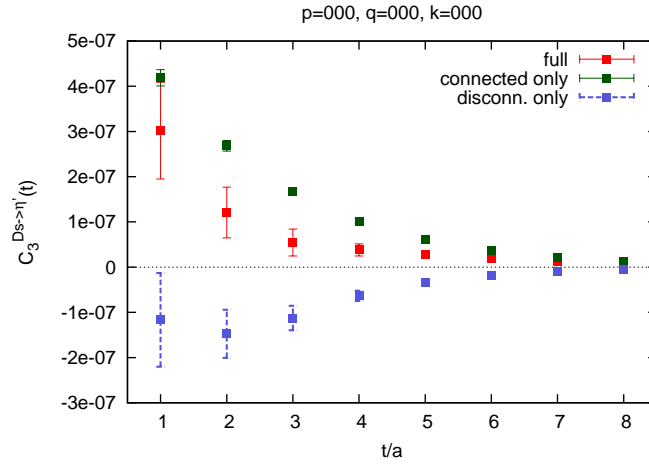


Figure 4: Connected and disconnected contributions to the three point function $C_3^{D_s \rightarrow \eta'}(t)$ with $\vec{p} = \vec{q} = \vec{k} = \vec{0}$ and $M_\pi = 348\text{MeV}$. The D_s meson is created at $t/a = 0$ and the η' is annihilated at $t/a = 8$.

4. Conclusions

We calculated the semi-leptonic decay form factors for $D_s \rightarrow \bar{l} \nu_l \eta$ and $D_s \rightarrow \bar{l} \nu_l \eta'$ using QCDSF $n_f = 2 + 1$ lattice configurations. This is the first lattice result of decay form factors which includes the fermion disconnected loop contributions. It turned out that the disconnected fermion loops give significant contributions to the form factor. The result is still preliminary but promising: the scalar form factor at zero momentum transfer $f_0(0)$ can be obtained with 10–15 % precision.

We are planning to use larger lattices and lower quark masses. Another target in addition to $f_0(q^2)$ is the other form factor $f_+(q^2)$. We are also interested in calculating the $D_s \rightarrow \bar{l} \nu_l \phi$ decay form factor that also contains a disconnected quark line contribution and the same calculation techniques are applicable.

Acknowledgements

This work was supported by the DFG SFB/TR 55 and the EU ITN STRONGnet. We used a modified version of CHROMA software suite [21]. The calculations were performed on the Athene HPC cluster and iDataCool at the University of Regensburg. It is my pleasure to thank my colleagues from the QCDSF collaboration for providing the configurations.

References

- [1] C. Di Donato, G. Ricciardi and I. Bigi, Phys. Rev. D **85** (2012) 013016 [arXiv:1105.3557 [hep-ph]].
- [2] J. Yelton *et al.* [CLEO Collaboration], Phys. Rev. D **80** (2009) 052007 [arXiv:0903.0601 [hep-ex]].
- [3] J. Yelton *et al.* [CLEO Collaboration], Phys. Rev. D **84** (2011) 032001 [arXiv:1011.1195 [hep-ex]].
- [4] H. Na, C. T. H. Davies, E. Follana, P. Lepage and J. Shigemitsu, PoS LAT **2009** (2009) 247 [arXiv:0910.3919 [hep-lat]].
- [5] K. Azizi, R. Khosravi and F. Falahati, J. Phys. G **38** (2011) 095001 [arXiv:1011.6046 [hep-ph]].
- [6] E. Witten, Nucl. Phys. B **156** (1979) 269.
- [7] G. Veneziano, Nucl. Phys. B **159** (1979) 213.
- [8] G. S. Bali *et al.* [QCDSF Collaboration], PoS LATTICE **2011** (2011) 283 [arXiv:1111.4053 [hep-lat]].
- [9] R. Evans, G. Bali and S. Collins, Phys. Rev. D **82** (2010) 094501 [arXiv:1008.3293 [hep-lat]].
- [10] G. S. Bali, S. Collins and A. Schäfer, Comput. Phys. Commun. **181** (2010) 1570 [arXiv:0910.3970 [hep-lat]].
- [11] W. Bietenholz *et al.* [QCDSF collaboration], Phys. Lett. B **690** (2010) 436 [arXiv:1003.1114 [hep-lat]].
- [12] W. Bietenholz *et al.* [QCDSF collaboration], Phys. Rev. D **84** (2011) 054509 [arXiv:1102.5300 [hep-lat]].
- [13] N. Cundy *et al.*, Phys. Rev. D **79** (2009) 094507 [arXiv:0901.3302 [hep-lat]].
- [14] S. Güsken, U. Löw, K. H. Mütter, R. Sommer, A. Patel and K. Schilling, Phys. Lett. B **227** (1989) 266.
- [15] N. H. Christ *et al.*, Phys. Rev. Lett. **105** (2010) 241601 [arXiv:1002.2999 [hep-lat]].
- [16] E. B. Gregory *et al.* [UKQCD Collaboration], Phys. Rev. D **86** (2012) 014504 [arXiv:1112.4384 [hep-lat]].
- [17] J. J. Dudek, R. G. Edwards, B. Joo, M. J. Peardon, D. G. Richards and C. E. Thomas, Phys. Rev. D **83** (2011) 111502 [arXiv:1102.4299 [hep-lat]].
- [18] K. Ottnad *et al.* [ETM Collaboration], JHEP **1211** (2012) 048 [arXiv:1206.6719 [hep-lat]].
- [19] F. Ambrosino, A. Antonelli, M. Antonelli, F. Archilli, P. Beltrame, G. Bencive JHEP **0907** (2009) 105 [arXiv:0906.3819 [hep-ph]].
- [20] M. Ablikim *et al.* [BES Collaboration], Phys. Rev. D **73** (2006) 052008 [hep-ex/0510066].
- [21] R. G. Edwards and B. Joó [SciDAC and LHPC and UKQCD Collaborations], Nucl. Phys. Proc. Suppl. **140** (2005) 832 [hep-lat/0409003].